

## Hough Transform for Target Identification from Linear Sensor Array F-K Spectrum

Jisha Kuruvilla P<sup>1</sup>, Kavitha Issac<sup>2</sup> and Neena Mani<sup>3</sup>

<sup>1</sup>Assistant Professor, EEE Department,  
M.A College of engineering, Kerala,  
[jishakuruvilla@yahoo.co.in](mailto:jishakuruvilla@yahoo.co.in)

<sup>2</sup>Assistant Professor, EEE Department,  
M.A College of engineering, Kerala,  
[kavithaissac@gmail.com](mailto:kavithaissac@gmail.com)

<sup>3</sup>Assistant Professor, EEE Department,  
M.A College of engineering, Kerala,  
[neenamani@yahoo.com](mailto:neenamani@yahoo.com)

### Abstract

Non-acoustic self-noise observed in towed sonar arrays represents a serious problem for acoustic source detection at low frequency. The decomposition of an array snapshot into its constituent acoustic and non-acoustic components is accomplished using a frequency-wavenumber, or F-K transform. Frequency-wavenumber diagrams can be used in order to differentiate between acoustic and non-acoustic noise. The frequency wavenumber transform is a double Fourier transform, both in time and in space, where the positive time frequencies are plotted along the y axis and the x axis represent the spatial frequency k. The acoustic energy is confined within the V-area of the F-K diagrams. Energy outside this V will highlight non-acoustic energy. From the f-k spectrum, target detection is possible using the principle of line detection by Hough transform. The Hough transform (HT), named after Paul Hough who patented the method in 1962, is a powerful global method for finding lines in an image. It transforms between the Cartesian space and parameter space.

**Key words--** Beamformer, Beam steering, FK transform, Hough Transform.

## INTRODUCTION

Beamforming is described as the coherent processing of an array of receivers in order to ascertain the arrival directions of the incident signals or to increase the signal- to- noise ratio of a signal from a given direction. “Forming beams” seems to indicate radiation of energy. However, beamforming is applicable to either radiation or reception of energy. Beamforming is a general signal processing technique used to control the directionality of the reception or transmission of a signal on a transducer array. Conventional beamforming can be done in time domain as well as in frequency domain.

In Time domain beam forming, time delayed and weighted sensor outputs are summed together to form beams in each steering direction. In frequency domain beam forming, weighted phase delay and sum technique is used for steering the beam in a given direction for each frequency bin. The array response is maximum when the direction of arrival (DOA) is on broad side ( $\Theta = 0$ ). The maximum, however, can be changed to any direction through a simple act of introducing a time delay to each sensor output before summation. This is known as array steering. In frequency domain beamforming the array is steered by delaying the incoming data with the help of a steering vector,  $s$ , and then performing a summation of the delayed outputs, thereby yielding the beamformer output. The steering vector is independent of the incoming data, and may be calculated a priori and stored in memory.

$$S(\theta) = \{1, e^{-j\omega d \sin(\theta)/c}, e^{-j\omega 2d \sin(\theta)/c}, \dots, e^{-j\omega(n-1)d \sin(\theta)/c}\} \quad (1)$$

Where  $\Theta$  is the direction of the steered beam and  $d$  is the distance between individual sensors. In figure 1, the time delay inserted on an impinging wavefront is denoted by

$$\tau = (d/c) \sin\theta \quad (2)$$

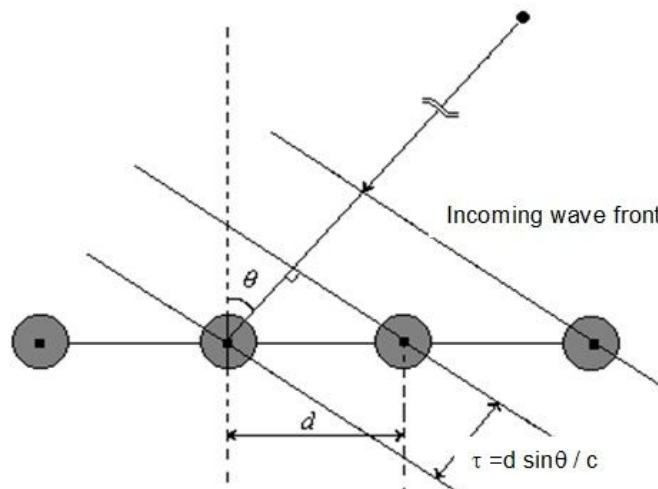


Fig.1. Schematic of linear array of hydrophones

Let  $x_n(i)$  denote the time series from the  $n^{\text{th}}$  hydrophone where  $n$  varies from 0 to  $N-1$ .  $N$  is the number of sensors and  $i$  is the time index of the sampled data. The time series from each sensor is segmented into blocks of length  $M$ , and the discrete Fourier transform (DFT) coefficients  $X_n(k)$  are computed. Here  $k$  is the frequency index and corresponding frequency being  $f_k = kf_s/M$ , where  $f_s$  is the sampling frequency. The beamformer output at a steering angle  $\theta$  and at frequency bin  $k$  is then given by

$$Y(k, \theta) = \sum_{n=0}^{N-1} W_n X_n(k) \exp[-j2\pi n f_k T(\theta)] \quad (3)$$

### F-K TRANSFORM

Conventional delay-sum beamformer depicts the scenario as bearing vs amplitude and it lacks the information on the temporal variation of the signal. For certain applications like torpedo detection, where a spatio-temporal view is required, frequency domain beamformer is employed. But the limitation of conventional frequency domain beamformer is its computational complexity. Here we present a method of generating another kind of spatio-temporal view for the linear array using Frequency-Wave number Transform (FK transform), which employs two-dimensional spectrum of a line array. This method is computationally less expensive and is faster than the conventional frequency domain beamformer since only the Fast Fourier Transform (FFT) operations are involved. The conventional spatio-temporal view can be generated from the FK transform by a simple look-up table method. Also the conventional bearing vs. amplitude view can be generated from the FK transform by line integration.

The F-K transformation is in principle a two-dimensional Fourier transformation. Corresponding to the transformation of the time-axis to the frequency domain, the x-axis is transformed to the wavenumber domain. The frequency indicates the number of oscillations per second. The Wavenumber  $k$  indicates the number of wavelengths per meter along the horizontal axis, for waves which propagate horizontally, the transformation returns the actual wavenumber. For waves that do not propagate horizontally, the horizontal component of the wave is transformed.

The plotting of a dataset in F-K domain is called an F-K spectrum. Analogous to the frequency spectrum for the one-dimensional transformation from time to frequency. The signals are separated and plotted as function of the frequency and wave number. The transform domains are shown in fig-2.

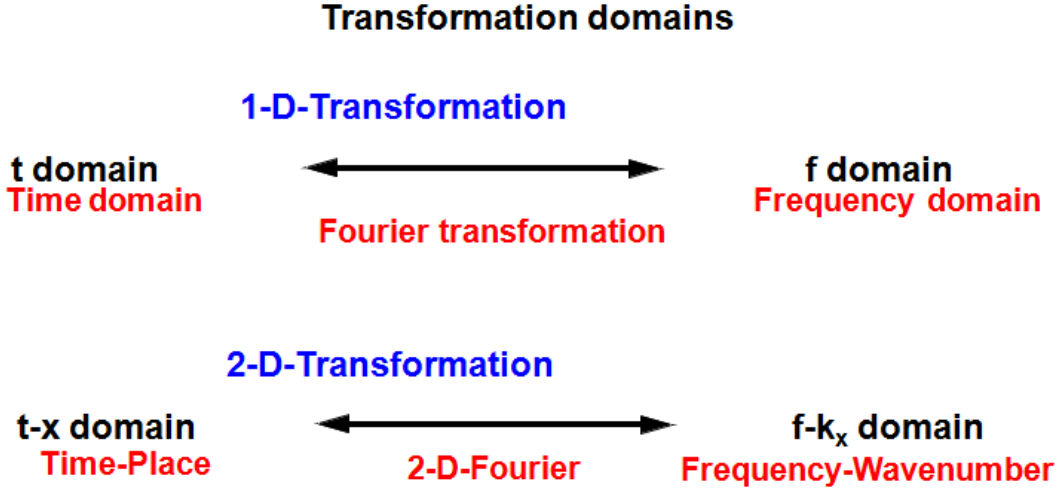


Fig.2. Transformation domains

### The frequency-wavenumber grid

Given an incident plane wave of frequency  $f$  and arrival angle  $\Theta$ , its spatial frequency, or wavenumber, as seen along the axis of the array is  $k \equiv (2\pi f/c) \sin\Theta$ . The units of wavenumber are inverse distance and so a normalized wavenumber  $k$  can be defined by

$$k = 2\pi f (d/c) \sin\Theta = \pi (f/f_d) \sin\Theta \quad (4)$$

Where  $f_d = c/2d$  is the design frequency of the array. Equation 5 is the basis for the frequency-wavenumber grid shown in figure 4. Lines of constant angle, as determined by this equation have been plotted in  $30^\circ$  increments. The shaded area of the grid is the non acoustic region, in which no waterborne acoustic signal can lie, and the diamond shaped area (with the dotted lines forming the top) is the region in which spatial aliasing cannot occur.

Note that below the design frequency, only a subset of the spatial FFT coefficients lie within the acoustic region. At the design frequency, however, all the samples are used, the fold over spatial frequency corresponding to either forward or aft end fire (this is the onset of spatial aliasing. At the design frequency, it is impossible to distinguish between an arrival at forward end fire and one at aft end fire. Steering angle  $\Theta_m$  for the  $m$ th bin is given by,

$$\Theta_m = \sin^{-1} \left( \frac{C_m}{f} N d \right) \quad (5)$$

within the acoustic region.

The FFT method, although computationally efficient, does not allow formation of beams at arbitrary steering angles, but only at those angles in equation 6. Furthermore, the steering angles of the beams it does form are

different at each frequency  $f_k$ . The evaluation of  $B(k, \Theta_m)$  is usually restricted to lines of constant bearing on the frequency-wavenumber grid, as shown in figure 3.

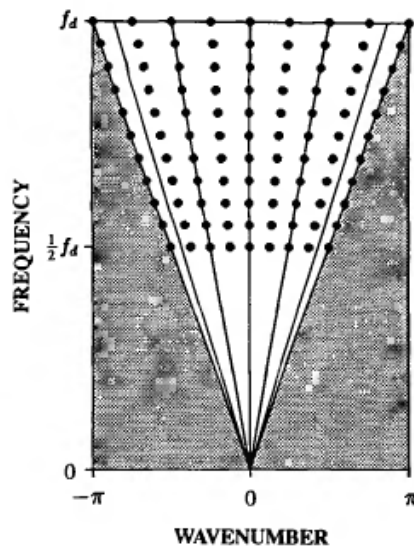


Fig. 3. Spacing of samples on lines of constant bearing on the frequency-wavenumber grid.

### Algorithms

There are two basic processing approaches, exact and approximate. The exact algorithms are those which, in the absence of numerical round off error, would yield the exact values of  $B(k, \Theta_m)$  for  $m=0, \dots, N_b-1$ . Since the number of sensors usually does not exceed 256 and modern array processors use high precision floating point arithmetic, the effect of round off can be ignored in the beamforming algorithms presented here. The approximate methods, as the name implies, compute approximations to the values  $B(k, \Theta_m)$ . The approximation accuracy is a design factor, a more accurate approximation requiring an increase in the computational load.

The zero-padded FFT method is implemented here. This is an approximate method. The idea behind this method is very simple, by extending the data with a large number of zeros before taking an FFT in the spatial dimension; the output samples are sufficiently dense on the frequency wavenumber grid that there will be a sample close to an arbitrary steering angle. Denoting the zero padding factor by  $P$  (i.e., an  $NP$ -point FFT is used instead of an  $N$ -point FFT), equation (6) is modified to give  $\Phi_m = \sin^{-1}(cm/f_k NPd)$ , for the exact steering angles within the acoustic region. By choosing  $P$  sufficiently large, one of the  $\phi_m$  will lie near any desired steering angle  $\Theta$ . As  $P$  is increased, the error in approximation between  $B(\Phi_m)$  and  $B(\Theta)$  is made smaller. The computational load is simply that of computing an  $NP$ -point complex FFT.

### F-K Transform simulation plots

In our simulation using MATLAB we considered a linear array with 32 elements with a target at  $45^0$  scenario. The input signal contains frequencies up to 2 kHz and the sampling frequency is chosen as 12800Hz. Sensors are spaced at corresponding to 2 kHz. Sound speed is taken as 1500m/Sec. F-K transform plots are given in fig-4. (a) is the frequency-wavenumber plot. (b) DOA vs Frequency energy plot. (c) DOA vs energy plot and (d) is the frequency vs amplitude plot in the target direction. Target was simulated for uniform energy for all frequency bins up to  $\lambda/2$ .

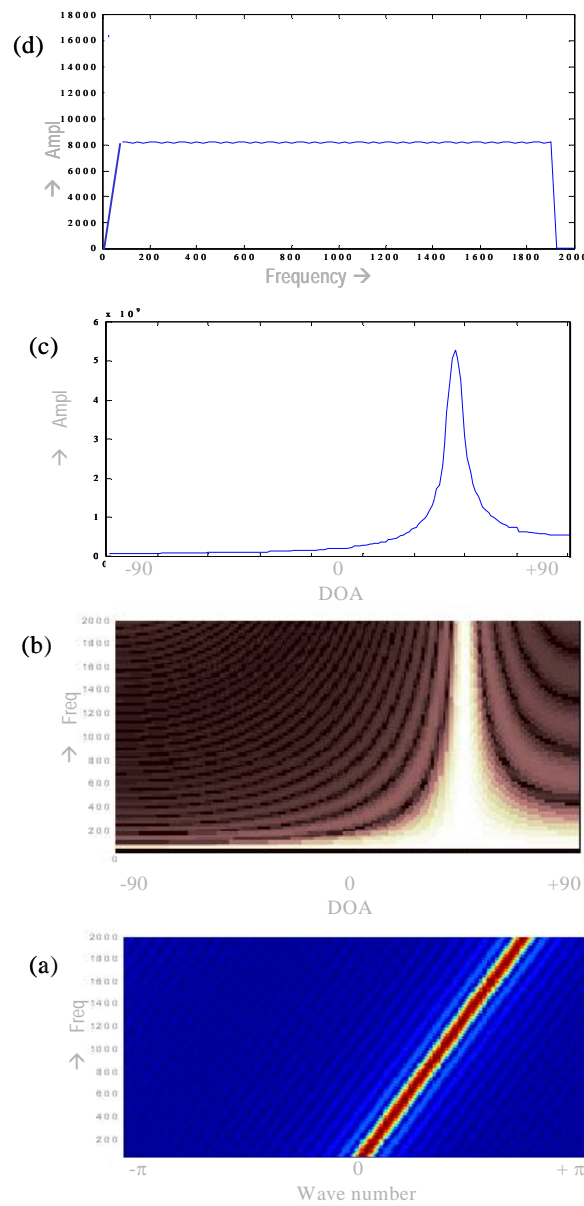


Fig. 4. F-K transform plots

### III. HOUGH TRANSFORM

The Hough transform is a feature extraction technique used in image analysis, computer vision, and digital image processing. The classical Hough transform was concerned with the identification of lines in the image.

The expression for a straight line is  $y=m*x+c$  (6)

Where  $m$  is the slope, and  $c$  is where the line intersects the  $y$ -axis. These parameters,  $m$  and  $c$ , can be used to represent a straight line as a single point  $(m, c)$  in the parameter-space spanned by the two parameters  $m$  and  $c$ . The problem by representing a line as a point in the  $(m, c)$  parameter-space is that, both  $m$  and  $c$  goes towards infinity when the line becomes more and more vertical, and thereby the parameter space becomes infinitely large. Therefore it is desirable to find another expression of the line with some parameters that have limited boundaries. It is done by using an angle and a distance as parameters, instead of a slope and an intersection.

If the distance  $\rho$  (rho) is the distance from the origin to the line along a vector perpendicular to the line, and the angle  $\theta$  (theta) is the angle between the  $x$ -axis and the  $\rho$  vector (see Figure (5)), Equation (6) can be written as:

$$y = -\frac{\cos\theta}{\sin\theta} * x + \frac{\rho}{\sin\theta} \quad (7)$$

The expression here, instead of  $m$  and  $c$ , is found by trigonometrical calculations. To get an expression of  $\rho$ , Equation (7) can be rearranged to:

$$\rho = x * \cos(\theta) + y * \sin(\theta) \quad (8)$$

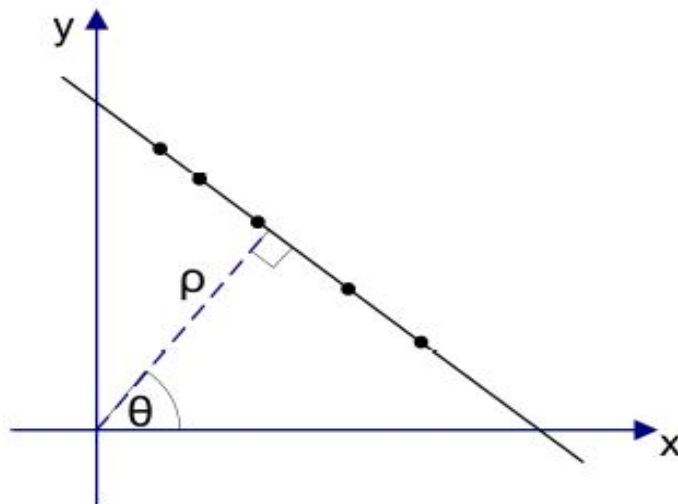


Fig. 5. Rho and theta representation of a straight line.

Contrary to, when the parameters is  $m$  and  $c$ , the values that  $\rho$  and  $\theta$  can have, are limited to:  $\theta \in [0, 180]$  in degrees or  $\theta \in [0, \pi]$  in radians, and  $\rho$

$\in [-D, D]$  where  $D$  is the diagonal of the image. A line can then be transformed into a single point in the parameter space with the parameters  $\theta$  and  $\rho$ , this is also called the Hough space.

The Hough space for lines has therefore these two dimensions;  $\theta$  and  $\rho$ , and a line is represented by a single point, corresponding to a unique set of parameters  $(\theta_0, r_0)$ . The line-to-point mapping is illustrated in figure 6.

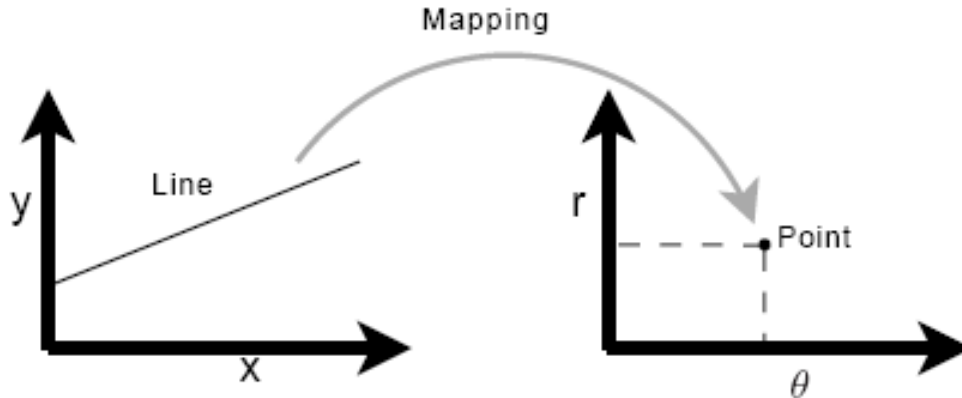


Fig. 6. Mapping of one unique line to the Hough space

### Mapping of points to Hough Space

An important concept for the Hough transform is the mapping of single points. The idea is, that a point is mapped to all lines that can pass through that point. This yields a sine-like line in the Hough space. The principle is illustrated for a point  $p_0 = (40, 50)$  in figure 7.

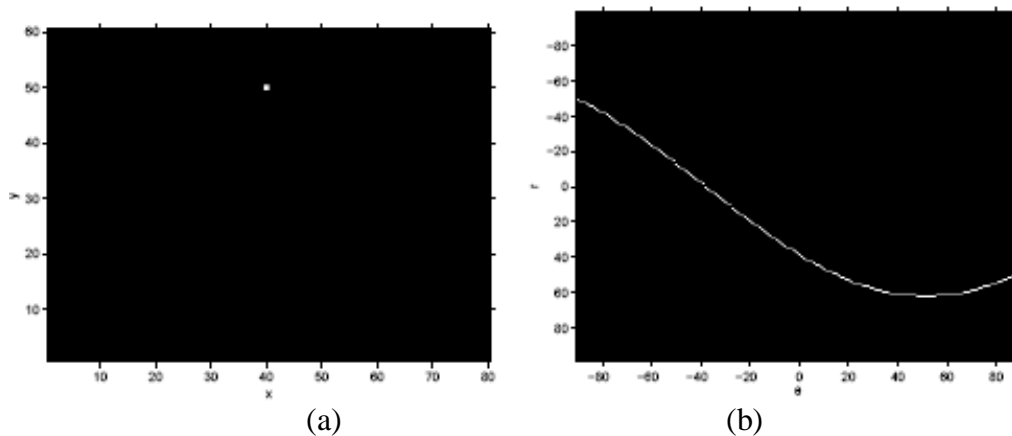


Fig.7. (a) Transformation of a single point ( $p_0$ ) to a line in the Hough space, (b) The Hough space line represents all possible lines through  $p_0$ .



**Target Detection By Hough Transform**

From the f-k spectrum, target detection is possible using the principle of line detection by Hough transform. Following the discussion above, we now can describe an algorithm for detecting lines in images. The steps are as follows:

1. Find all the edge points in the image using any suitable edge detection scheme.
2. Make available a two dimensional array  $H(\rho, \theta)$  for the parameter space.
3. Each element of  $H$  matrix, which is found to correspond to an edge point, is incremented by one. The result is a histogram or a vote matrix showing the frequency of edge points corresponding to certain  $(\rho, \theta)$  values (i.e. points lying on a common line).
4. The histogram  $H$  is thresholded where only the large valued elements are taken. These elements correspond to lines in the original image.

**Hough Transform: simulation results**

FK spectrum for a single target located at an angle of  $60^\circ$  is shown in fig (a). After thresholding, FK image will be obtained as in fig (b). Edge detected image is shown in fig(c). Hough transform of the edge detected image is computed. The result of the Hough transform is stored in a matrix often called an accumulator. One dimension of this matrix is the theta values (angles) and the other dimension is the rho values (distances), and each element has a value telling how many points/pixels that lie on the line with the parameters (rho, theta). So the element with the highest value tells which line is most represented in the input image. This (rho, theta) values will represent a curve in the parameter space. All curves will meet at a single point in the parameter space, if the points which map in to that curves are on the same line. Hough space of the edge detected image is obtained as in fig(d).

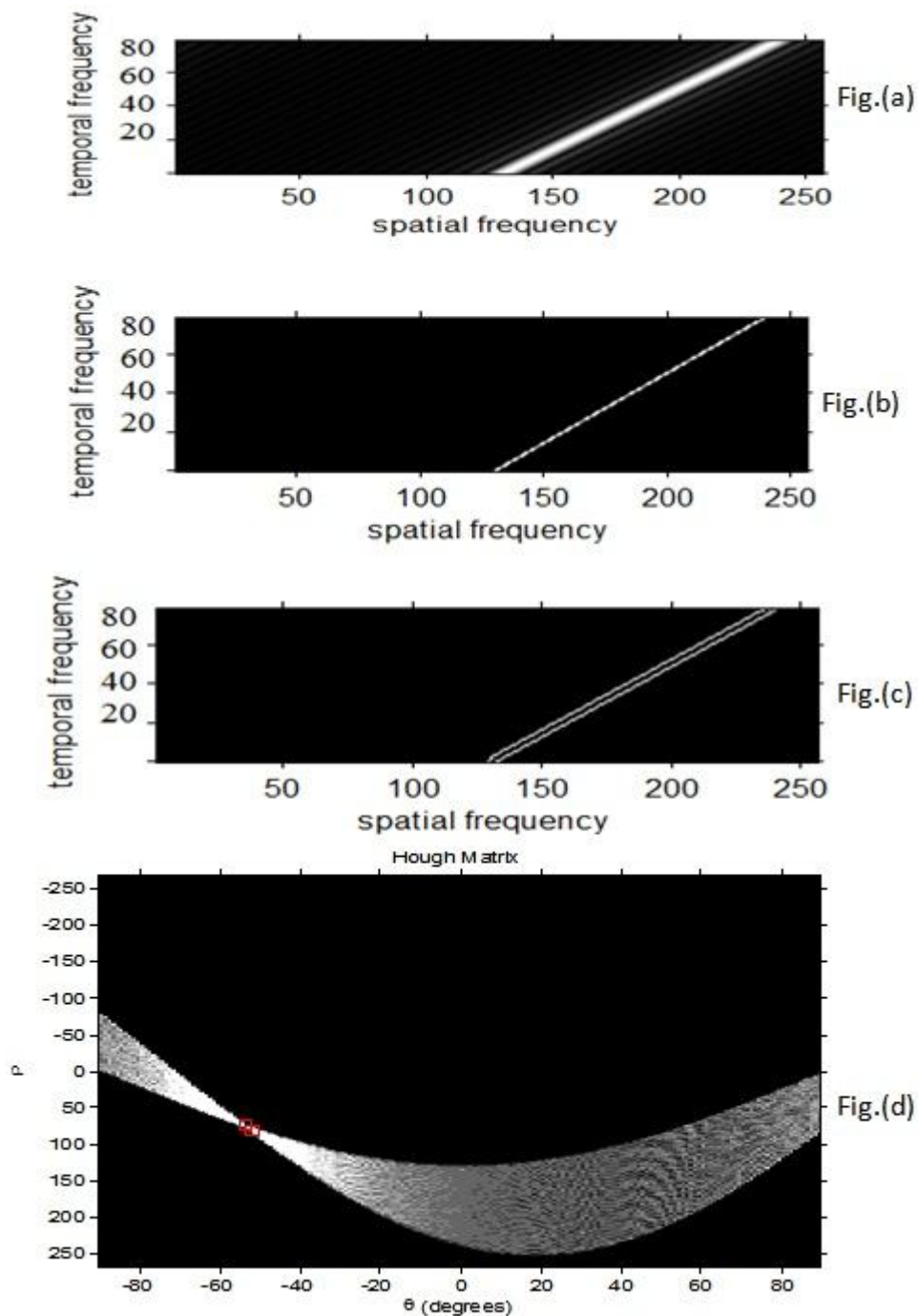


Figure 8: Simulation plots

### Non-Acoustic noise DETECTION using F-K transform

A sonar array towed through a water medium typically generates non-acoustic noise referred to as non-acoustic self noise. Self noise is generally due to mechanical vibrations induced by hydrodynamic flow over the array sensors as

the array is towed through the medium in which it is disposed. The vibrations propagate as transverse and longitudinal modes in the array body, much like a vibrating string with fixed boundary conditions. The vibrations produce local accelerations at each sensor. The acoustic response induced by this phenomenon can be several orders of magnitude stronger than that of acoustic signals propagating through the water column.

Thus, non-acoustic self noise observed on sonar towed arrays can unnecessarily prevent the detection and discrimination of acoustic signatures at low frequency, and thus can impose limits on system performance beyond those implied by the ambient acoustic noise environment.

The decomposition of an array snapshot into its constituent acoustic and non-acoustic components is accomplished using a frequency-wavenumber, or F-K transform. Frequency-wavenumber diagrams can be used in order to differentiate between acoustic and non-acoustic noise. These diagrams allow the identification of the speed of the pressure waves measured by the array. The acoustic energy is confined within the V-area of the F-K diagrams. Energy outside this V will highlight non-acoustic energy (mechanical vibrations, flow noise, etc). The borders of the V-shape represent the end fire beams energy.

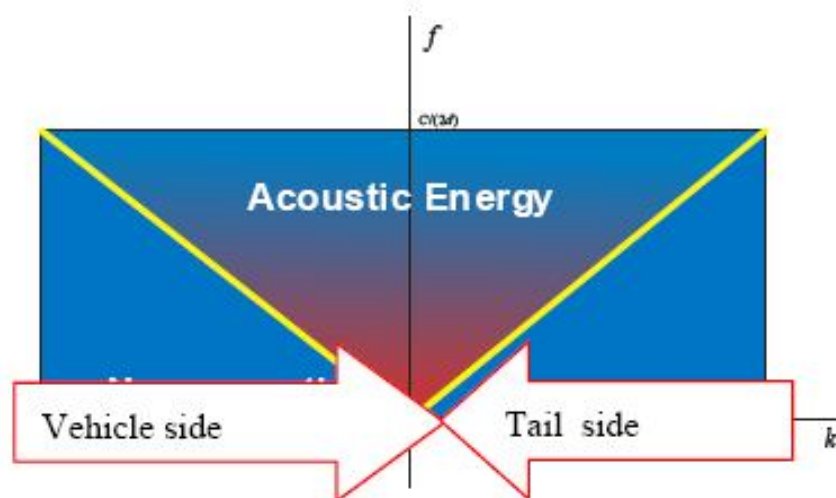


Fig. 9. F-K diagram and V-shape

The approach is based on the recognition that most vibrational modes of a towed array propagate at phase speeds substantially less than those of acoustic signals in the water column. The approach eliminates the need for additional measurement channels, such as accelerometers or strain gauges, to independently sense the undesirable distortions introduced by cable strumming. The phenomenology underlying flow-induced self-noise for towed arrays is discussed and characterized using F-K analysis. Here we utilize the characteristic feature of the F-K spectrum that effectively discriminates between normal sound waves and slow waves.

### Non-acoustic noise detection: simulation results

In MATLAB simulation we considered a linear array with 32 elements with targets at  $0^\circ$  and  $30^\circ$ . Sound speed is taken as 1500m/Sec for target at  $0^\circ$  and 500m/Sec for target at  $30^\circ$ .  $30^\circ$  target is simulated as a non-acoustic target. F-K transform plot is given in fig-10. Acoustic and non acoustic regions are marked in the figure. Target markings indicated inside the non-acoustic region indicates the presence of non-acoustic noise. Target with velocity 500m/s goes out of the boundary

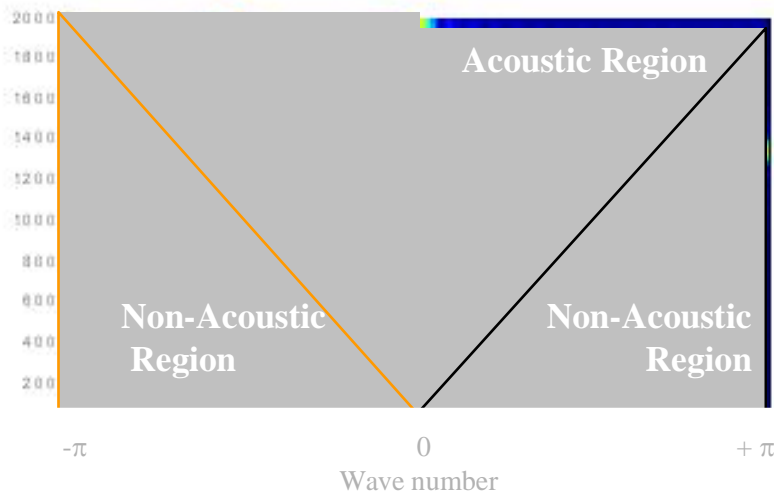


Fig. 10 Non-acoustic target marking in F-K spectrum

### REMOVAL OF NON-ACOUSTIC NOISE

The mapping from parameter space to image space is an inverse mapping procedure. Here, first we find out the local maxima in the accumulator space. By finding the bins with the highest values, typically by looking for local maxima in the accumulator space, the most likely lines can be extracted. The aim is to find out the  $(x, y)$  values for this  $(\rho, \theta)$  values. We can calculate all  $y$  values for  $x$  values in the image space. This calculation is based on the equation,

$$y = -x \cot \theta + \frac{\rho}{\sin \theta}$$

Using these  $(x, y)$  values, we can reconstruct the original image. With the help of the reconstructed image, we can mask the portion of the FK spectrum which lies outside the f-k plane. Thus, the non-acoustic energy can be removed. Also, presence of a target which lies within the f-k plane, has been properly detected.

### Removal of non-acoustic noise: simulation results

FK spectrum of two targets is shown in fig (a), one that lies outside the FK

plane is the non acoustic signal. The corresponding beam plot is shown in fig (b).After thresholding image is obtained as shown in fig(c).Edge detected image is shown in fig (d). Hough space of the edge detected image is shown in fig(e).Using the inverse mapping procedure, we can reconstruct the original image, which is shown in fig.(f).The reconstructed image is shown in fig (g).From the beam plot shown in fig (h) it is evident that non-acoustic energy is removed and what is remaining is the target signal.

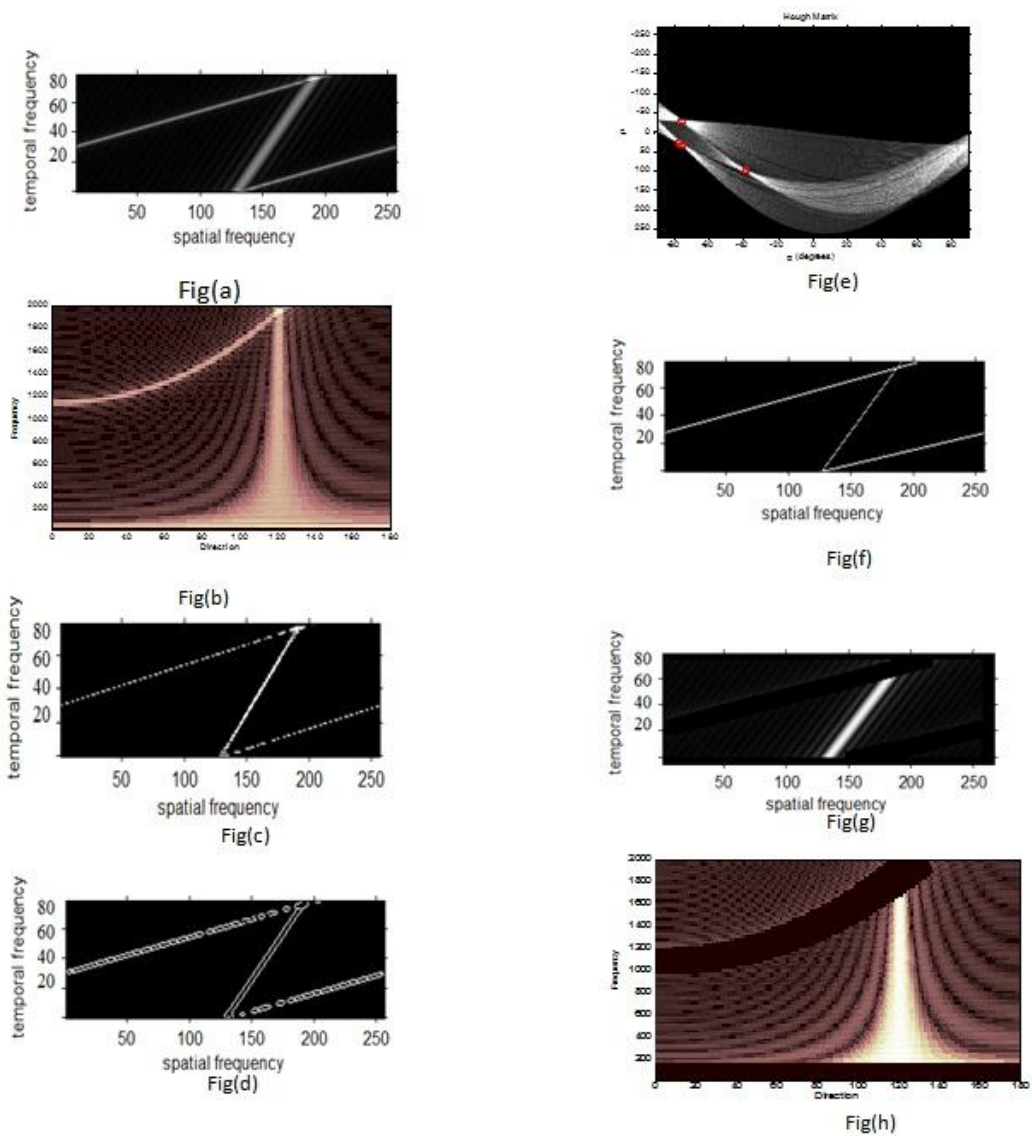


Fig.11. FK spectrum of two targets

**CONCLUSION**

F-K transform has been implemented for differentiating between acoustic and non acoustic energy. The phenomena underlying flow-induced self-noise for

towed arrays is discussed and characterized using F-K analysis. The performance is evaluated for both simulated and recorded data. Targets lying outside the F-K plane are detected and masked, by Hough Transform, enabling precise detection of the actual targets. Target detection using F-K transform is able to give an equivalent performance, as the normal time domain beamforming method, in terms of signal to noise ratio. The approach eliminates the need for additional measurement channels, such as accelerometers or strain gauges, to independently sense the undesirable distortions. This can be considered as a stepping stone for future implementations.

### **Acknowledgements**

Authors are immensely grateful to all those who have helped us directly or indirectly towards the successful completion of the paper.

### **References**

- [1] Barry.D.Van Veen and Kevin.M.Buckley, April 1988, 'Beamforming, a versatile approach to spatial filtering', IEEE ASSP Magazine.
- [2] Brian Maranda, 'Efficient digital beamforming in the frequency domain', Journal of Acoustical Society of America, vol 86, No 5, November 1989.
- [3] Johan Fredrik, Sverre Holm, Austeng, 2008, "A Low Complexity Data Dependent Beamformer, "IEEE International Ultrasonic's Symposium Proceedings.
- [4] G.L.Demuth, 1977, 'Frequency domain beamforming techniques', IEEE International Conference Acoustics, Speech and Signal Processing, page 713-715.
- [5] Prabhakar.S.Naidu, 2001, 'Sensor array signal processing', CRC Press, 1<sup>st</sup> Ed..